Plasma Science and Technology

PAPER

Hefei utility negative ions test equipment with RF source: commissioning and first results

To cite this article: Jianglong WEI *et al* 2018 *Plasma Sci. Technol.* **20** 125601

Plasma Sci. Technol. **20** (2018) 125601 (7pp) https://doi.org/10.1088/2058-6272/aadc06

Hefei utility negative ions test equipment with RF source: commissioning and first results

Jianglong WEI (韦江龙)[1], **Yahong XIE** (谢亚红)[1], **Caichao JIANG** (蒋才超)[1,2], **Lizhen LIANG** (梁立振)[1], **Qinglong CUI** (崔庆龙)[1], **Shiyong CHEN** (陈世勇)[1], **Yongjian XU** (许永建)[1], **Yan WANG** (王艳)[1,2], **Li ZHANG** (张黎)[1,2], **Yuanlai XIE** (谢远来)[1] **and Chundong HU** (胡纯栋)[1,2]

[1] Institute of Plasma Physics, Chinese Academy of Sciences, Hefei 230031, People's Republic of China
[2] University of Science and Technology of China, Hefei 230026, People's Republic of China

E-mail: xieyh@ipp.ac.cn

Received 29 March 2018, revised 2 August 2018
Accepted for publication 13 August 2018
Published 20 September 2018

Abstract

In order to study the key technology and physics of RF driven negative ion source for neutral beam injector in China, the Hefei utility negative ions test equipment with RF source was developed at Institute of Plasma Physics, Chinese Academy of Sciences (ASIPP). Its negative ion source can be equipped with single or double RF drivers. There is a plasma expansion chamber with depth of 19 mm and an enhanced filter field. A three electrodes negative ion accelerator was employed to extract and accelerate the negative ions, which are plasma grid, extraction grid and ground grid. And there are several diagnostic tools for the plasma and beam parameters measurement. The characteristics of plasma generation, negative ion production and extraction were studied on the test equipment. The negative ion beam was extracted from the RF driven negative ion source for the first time. The detailed structure and main results are presented in this article.

Keywords: neutral beam injection, negative ion source, CFETR, negative ions extraction

(Some figures may appear in colour only in the online journal)

1. Introduction

The China Fusion Engineering Test Reactor (CFETR) is a new fusion facility, which aims to bridge the gap between ITER and fusion demonstration reactor (DEMO) and to realize the fusion power in China [1–4]. Neutral beam injection (NBI) is one of the proposed heating and current driver systems for magnetic confinement fusion devices. According to the latest physics design of CFETR, a deuterium neutral beam above 0.8 MeV is demanded to support the current drive and the plasma rotation. At that high beam energy, the common positive ion source is not adequate due to a limited neutralization efficiency below 10%, but the negative ion source can still achieve a neutralization efficiency nearly 60% [5]. However, the challenge is the negative ions are harder to generate and to handle than the positive ions [6]. The positive ions can be directly produced through the gas discharge by energetic electrons, while the generation of negative ions is a multi-stage process (via the vacuum process or the surface process) where the gas discharge is just the precondition. The extraction and acceleration of negative ions is also more complex than that of positive ions, on the problems of the low extracted negative ion current density, the co-extraction of electrons, the high stripping loss of negative ions, and so on. Thus, the negative ion source has been one of the most critical issues in the NBI R&D for decades [7–13]. Similarly, a prototype negative NBI system of CFETR device will be developed in China during the next 5 years.

Before the practice of the CFETR prototype injector, the Hefei utility negative ion test equipment with RF source was developed at Institute of Plasma Physics, Chinese Academy of Sciences (ASIPP) [14]. The test equipment comprises

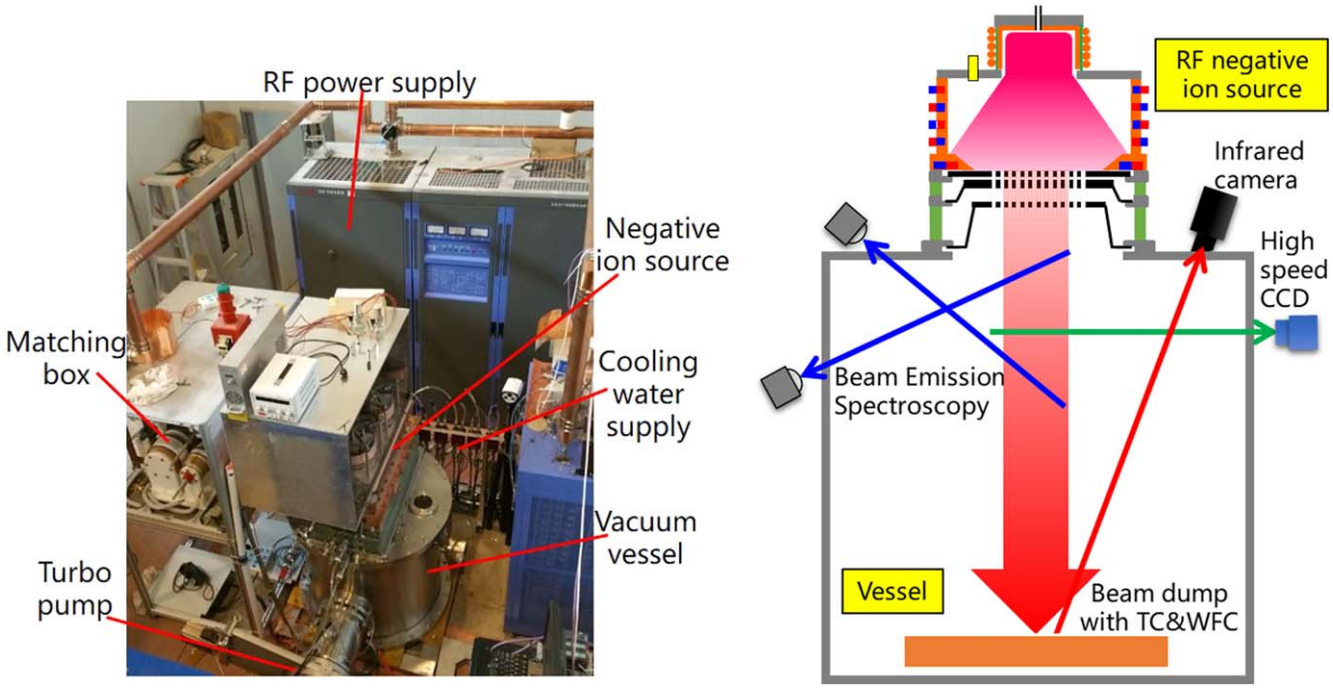

Figure 1. The picture and the sketch of Hefei utility negative ion test equipment with RF source at ASIPP.

negative ion source, vacuum vessel and auxiliary system, power supply system, diagnostics system, and control and data acquisition system (as shown in figure 1). Its negative ion source has a similar structure with that of CFETR prototype injector, but the size is about one-fourth. Its mission is to understand the characteristics of the RF source operation and the negative ions generation and extraction and to improve the RF efficiency and the beam quality. Although the acceleration voltage and the beam duration are limited due to the capability of the power supply and the pumping system, it is flexible to test and to compare different concepts (e.g., different magnetic filter field, different co-extracted electron deflection magnetic field, different electrode aperture shape) with kinds of diagnostic techniques. Hence, the test equipment can be utilized to optimize the physics design of the CFETR prototype injector and minimize the risks of the unsuccessful operation.

After two years of construction and assembly, the test equipment has been commissioned since May 2017. Considered a stable plasma discharge is the guarantee of negative ions generation, the high-power and low-pressure RF plasmas were firstly achieved [15, 16]. The whole power supply system [17] was debugged at the same time, including the RF plasma discharge with isolating transform and the extraction voltage based on a dummy load. And then, the negative ions were tried to be extracted without cesium seeding, where the negative ions were generated through the dissociations of the excited hydrogen molecules H_2^* (called vacuum process) and the yield of negative ions was low. The details of the first extraction experimental results are described in this article.

2. System description

Due to the achievements of the BATMAN and MANITU test facilities at IPP-Garching [18–21], they were taken as references during the design process of the test equipment here. Besides, several mature techniques or instruments from the EAST NBI system [22] were applied to the test equipment. It is designed to allow a flexible diagnostic access and a utility application to different design concepts.

The details of the negative ion source are described in [23]. As shown in figure 2, it can be equipped one or two RF drivers in which the plasma is generated through inductive coupling. A 1 MHz RF generator is applied to supply the RF power of 50 kW. The plasma generated in the driver then expands into the plasma chamber of 65 cm (L) $\times$ 26 cm (W) $\times$ 19 cm (H). A magnetic filter with two rows of permanent magnets divides the plasma chamber into expansion region and extraction region [24]. It is used to suppress the negative ion destruction by hot electron collisions and to reduce the co-extracted electrons meanwhile [25–27]. To generate sufficient hydrogen negative ions and to reduce the amount of co-extracted electrons, the cesium is evaporated into the source to produce the negative ions via the surface conversion process [28–30].

The hydrogen negative ions can be extracted and accelerated up to 10 + 50 kV by the accelerator. The extraction voltage power supply and acceleration voltage power supply are independent. The beam extraction and acceleration systems comprise three grids: the plasma grid (PG), the extraction grid (EG) where the co-extracted electrons are deflected out of the beam by embedded permanent magnets, and the ground grid (GG) [31, 32]. Each grid is divided into 4 segments

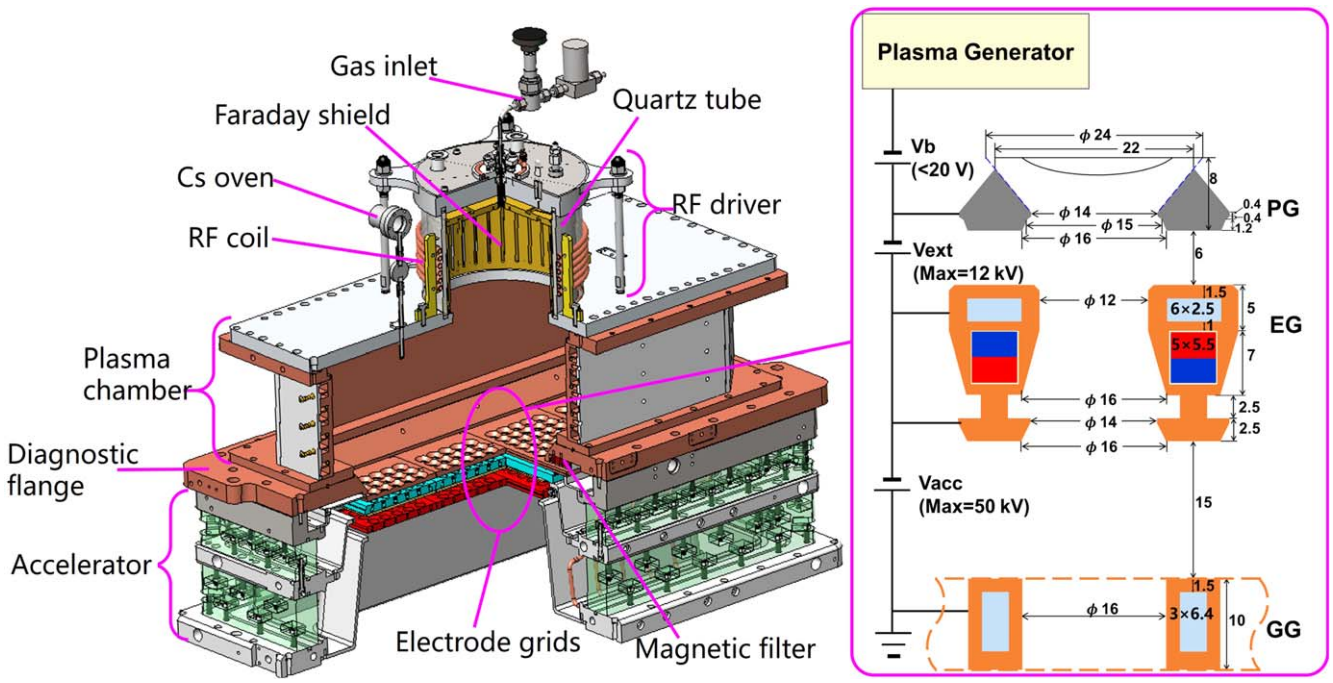

Figure 2. The 3D diagram of the negative ion source and the detailed geometry of the grid aperture. The distance units in all the figures of this article are mm.

Table 1. Diagnostic system for the test equipment.

	Diagnostic tool	Parameter
Source diagnostics	Langmuir probe (LP)	T_e, n_e, n_{H+}, V_p, plasma uniformity
	Optical emission spectroscopy (OES)	n_{Cs}, $n_{impurity}$, T_e, n_e, n_{H0}
	Cavity ring-down spectroscopy (CRDS)	n_{H-}
	Thermocouple (TC)	Temperature of source walls and PG
	Calorimetry	RF power transfer efficiency
Beam diagnostics	High-speed CCD	Beam profile
	Beam emission spectroscopy (BES)	Beam divergence, stripping loss
	Infrared camera (IR)	Beam divergence and uniformity
	Thermocouple (TC)	beam divergence and uniformity
	Calorimetry with beam dump	J_e/J_{H-}, beam power

and each segment has 5 × 6 apertures. The aperture geometry of the grid system is based on the design of ITER NBI ion source. The extraction area is 184 cm^2 (i.e., the total area of the apertures on the PG). To suppress the ratio between co-extracted electrons and negative ions, the PG is positively biased against the plasma generator [33–35]. Long-pulse RF plasma discharge is feasible up to 1000 s, but the extraction pulse is under 10 s at the moment due to the limitation of the pumping system.

The test equipment is equipped with several source and beam diagnostics, as listed in table 1. The key parameters of source plasma are mainly measured through the ports on a diagnostic plate close to the PG. This plate is also used as the bias voltage plate. In addition, some diagnostic ports on the back plate of plasma chamber can be utilized during the single driver operation. The high-speed CCD is used for the beam monitoring during the operation. Whereas the quantitative beam parameters such as divergence and uniformity are obtained from the beam emission spectroscopy [36] using 2 lines-of-sight and a dedicated diagnostic beam dump with infrared camera and thermocouple array [14].

3. Experiment results

3.1. Basic RF operation

A stable, high-density and uniform plasma is necessary for the negative ions generation and extraction. The R&D on RF plasma discharge was carried out step by step. Firstly, the single RF driver and the matching network was tested via a plasma chamber without accelerator. Besides the common start filament method, a pressure control method was also used for plasma ignition, where a high-pressure gas was injected at the beginning of discharge for ~1 s.

Secondly, the high-power RF plasma discharge was pursued at a low-pressure below 0.3 Pa. The low-pressure

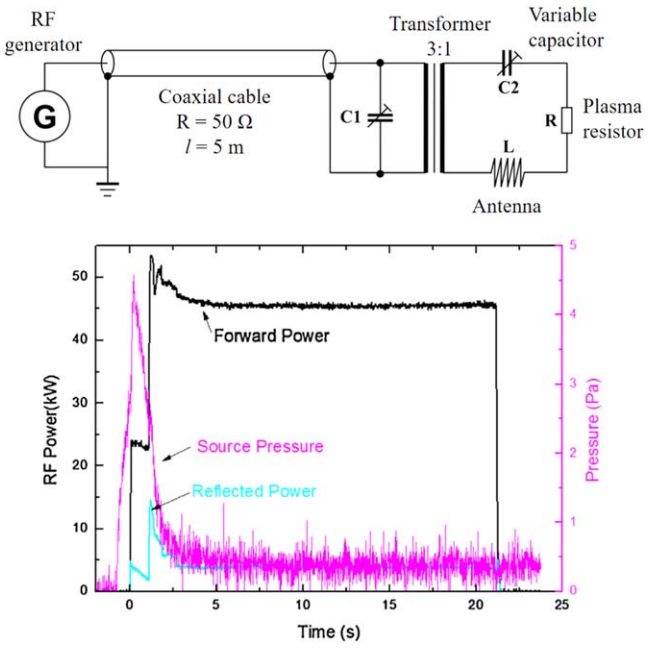

Figure 3. The matching network for RF operation and a typical waveform of RF plasma discharge.

operation was specially required for the negative ion beam source to minimize the stripping loss in the accelerator [37, 38]. Consequently, the stable and repeatable RF plasma discharge was achieved, with the incident power of >45 kW for ~10 s. The reflected power could be controlled under 5% of the incident power.

Thirdly, the plasma discharge duration was further extended up to 1000 s. But the obtained discharge power was limited to 10 kW during the long-pulse operation because the power deposition on the Faraday shield was extremely high. From the water-flow calorimetry results, the heat load on the Faraday shield was around 50% of the incident power. Thus, the current cooling design of Faraday shield had to be upgraded. The Faraday shield is installed inside the low dielectric tube to protect it against the plasma heat load. A design of the water-cooled tube is under development to avoid using the Faraday shield [39].

Finally, the isolation transformer and the accelerator were installed for the RF plasma discharge, to determine the final design parameters of the matching network. The major difference is the capacitor C1 was reduced from 19 to 4 μF with the transformer. A typical waveform of the RF plasma discharge is shown in figure 3.

3.2. Diagnostic system

An optical emission spectroscopy (OES) diagnostic system is designed and employed to measure and optimize the source plasma parameters, such as cesium density, impurity density, and electron density and temperature [40]. For single RF driver operation, a special OES system is installed on the back plate of the plasma chamber. A periscope-like structure is inserted into the chamber, to form the line-of-sight at different depths. In addition, a collisional-radiative (CR) model is used to calculate plasma parameters according to the emission spectrum [41]. A little of argon and xenon gas (5% of total injection rate) is puffed in the RF driver as the diagnostic gas. It has been routinely applied to the basic RF operation, not only during the studying shots, but also during the cleaning shots and conditioning shots. Especially during the initial testing, it is quite qualified for measuring the plasma features at different operative conditions. The results based on CR model under the same source pressure are shown in figure 4. The line-average electron temperature and electron density is about 4.5 eV and 3.5 $\times$ 10^{17} m^{-3} near the RF driver opening. The measured values of OES are verified via a commercial Langmuir probe (ESPion advanced Langmuir probe manufactured by Hiden analytical company). The Langmuir probe was installed on the diagnostic plate and the accelerator was not equipped during the verification. The measured electron temperature and density via OES have the same order of magnitude with that via Langmuir probe. The measuring point of Langmuir probe is ~15 cm downstream the sight of light of OES. Due to the diffusion effect, the measured values via Langmuir probe are a bit less than that via OES.

The cavity ring-down (CRD) is one of the laser absorption spectroscopies and a very sensitive detection technique for measuring small absorptions [42]. The line averaged density of absorber can be derived from the difference of decay times of laser signal with and without absorber. In the source plasma, the negative ions are the major cause for the laser absorption by the photo-detachment process. Thus, the CRD diagnostic system of the test equipment is the major measuring technique for hydrogen negative ion density (shown in figure 5). It consists of the vacuum cavity with two high-reflectivity mirrors, the laser light path and the matching detection and analysis system. A pulsed Nd:YAG laser is selected and the wavelength is 1064 nm. The reflectivity of the two mirrors is 99.999%. A photomultiplier tube is placed behind one mirror. The length of the cavity is 1.2 m and the length of the plasma region is supposed to be 0.6 m. The typical CRD detection signals with and without the source plasma are shown in figure 5. The ring-down duration is 20.317 μs and 23.516 μs with and without the source plasma, respectively. The calculated negative ion density is 5.2 $\times$ 10^{15} m^{-3} when the RF discharge power is 22 kW and the source pressure is 0.4 Pa.

3.3. Negative ions extraction

The grid conditioning was carried out firstly without Cs seeding. Because the high voltage power supply for the negative ions acceleration was under maintenance, the negative ions were extracted only by the EG power supply. Considered the large beam divergence with extraction only, a beam dump was installed on the GG supporting frame. Such an experiment design learned from the negative ion beam extraction experiment of JT-60SA negative ion source [30]. The circuit topology of this experiment is shown in figure 6. The extraction voltage was applied between the PG and the EG. The EG and the beam dump were shorted. According to the beam optics analysis, the sensing resistors R1, R2 and R3 were added in the circuit, to measure the drain current of the EG power supply, the co-extracted electron current and the

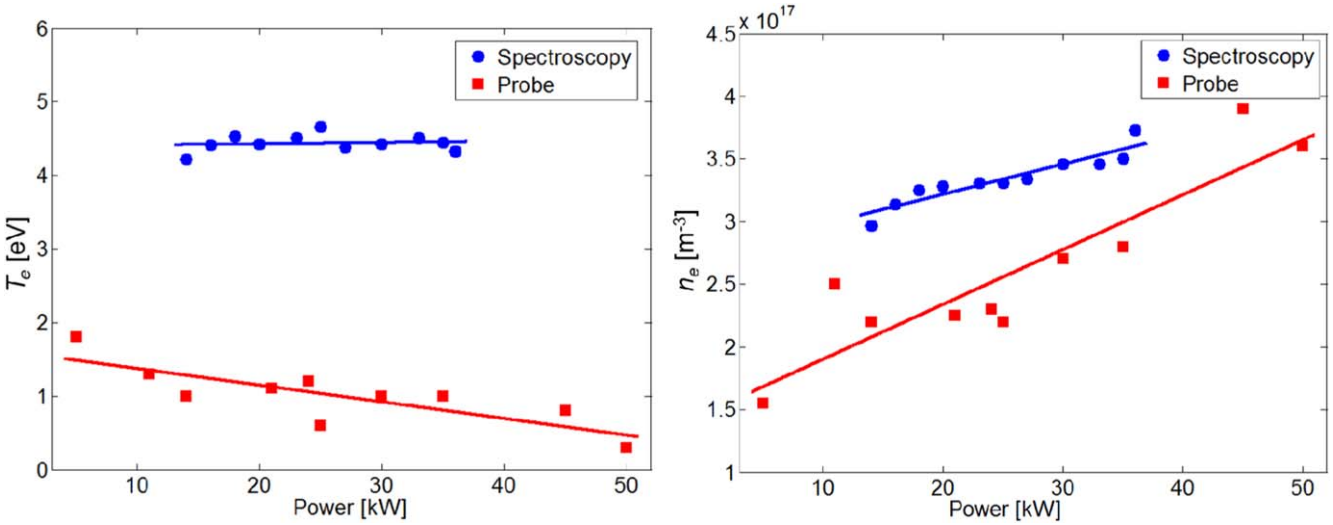

Figure 4. The variation of the electron temperature and electron density with RF power measured via OES and Langmuir probe.

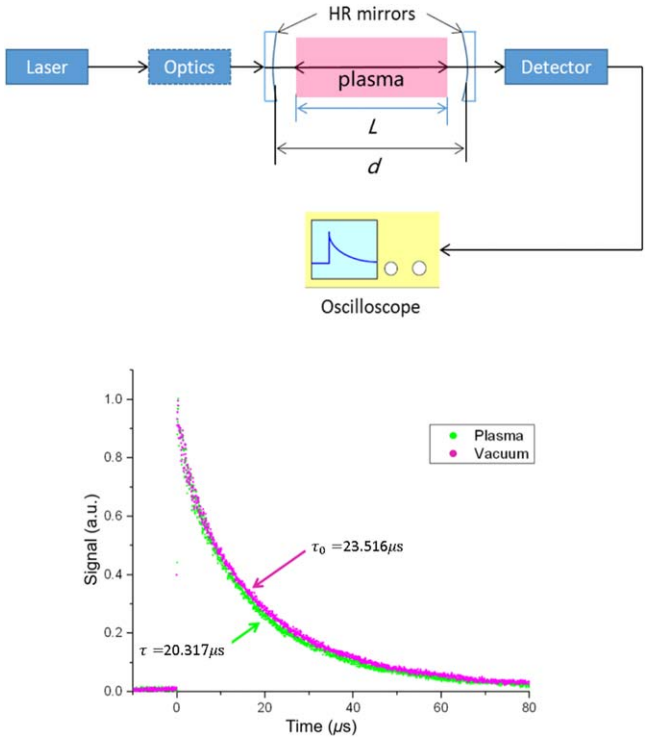

Figure 5. The typical CRD detection signals without and with plasma.

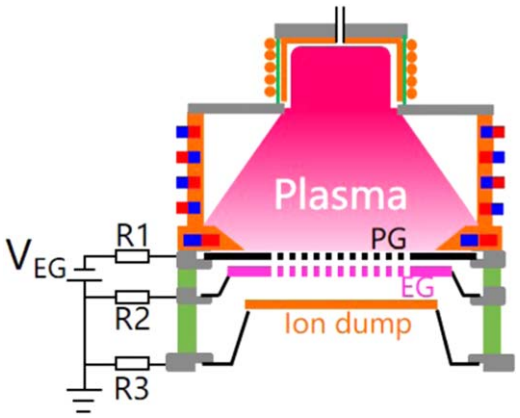

Figure 6. The circuit topology of the preliminary experiment of negative ions extraction.

extracted negative ion current, respectively. At the same time, the RF plasma discharge with double RF drivers was tested during the experiment.

During the grid conditioning, the source pressure was 0.5–0.8 Pa and the RF discharge pulse before the extraction was 2–3 s. The RF loaded power (= forward power − reflected power), the extraction voltage, and the extraction pulse were gradually increased. The impedance matching of the RF power was a key factor in achieving the efficient grid conditioning, and the typical waveforms are shown in figure 7. In the shot No. 3953, the RF forward power was 22 kW but the reflected power was high to 4 kW causing by an unsuitable impedance matching. The plasma was ignited by the start filament, so the gas was puffed in 5 s ahead of the RF power supply turning on. The extraction voltage was –6.9 kV. The drain current was 91.9 mA, the co-extracted electron current was 79.6 mA, and the negative ion current was 10.6 mA. Each current signal had a large fluctuation, which was induced by the mis-matching RF plasma discharge. Consequently, the beam extraction was stop at 1 s even though the set value of beam pulse was 2.5 s. For comparison, a shot with low reflected power (No. 3982) is also shown. The RF forward power was 17 kW and the reflected power was only 0.5 kW. Under this condition, the ripples of drain current and co-extracted electron current were obviously smaller.

The experimental results indicated that the drain current, the co-extracted electron current, and the extracted negative hydrogen current were increased with the RF loaded power and the extraction voltage, as indicated in figure 8. The highest negative hydrogen current was above 10 mA. The

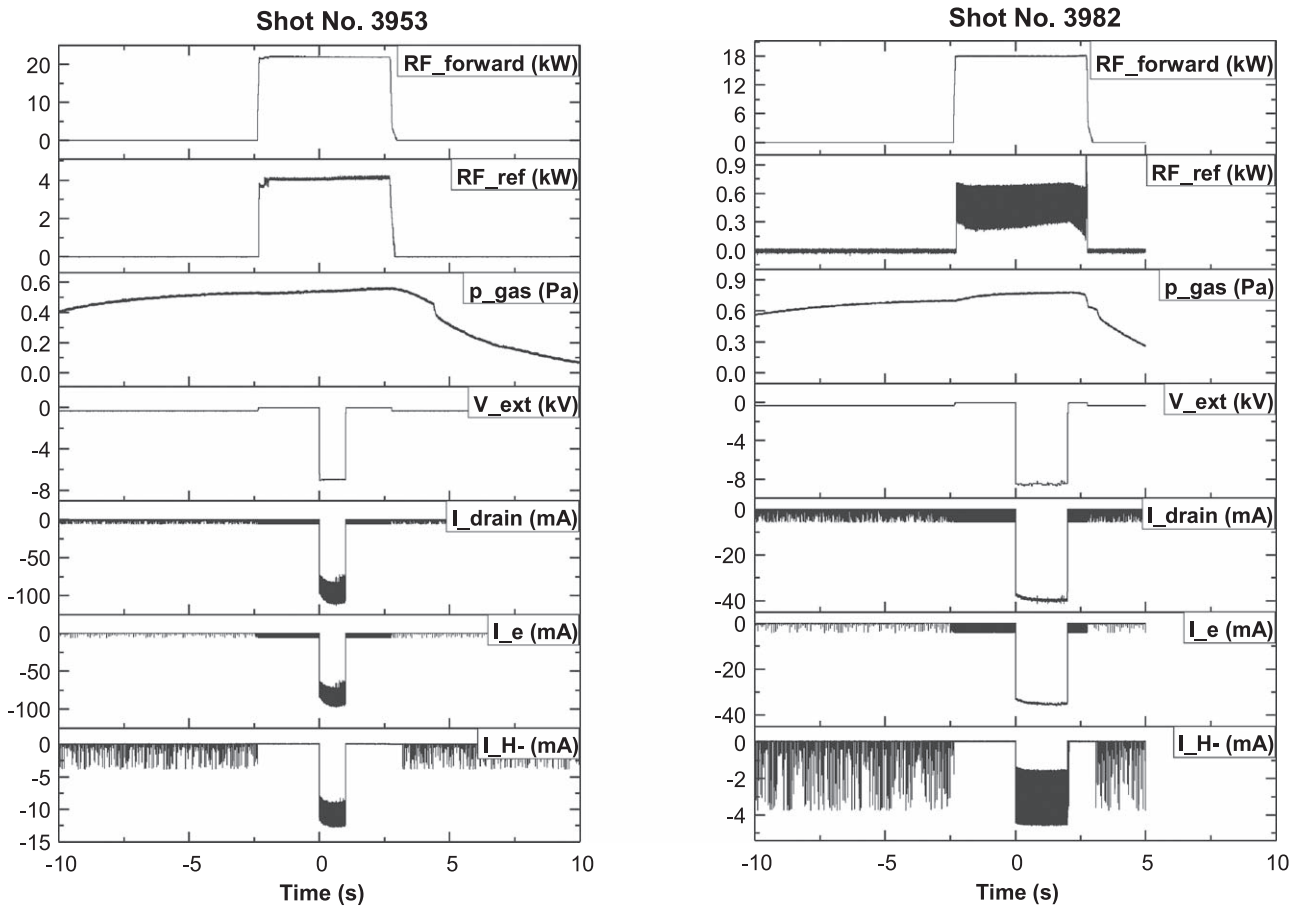

Figure 7. The typical waveforms of the negative ions extraction with high (No. 3953) and low (No. 3982) RF reflection power.

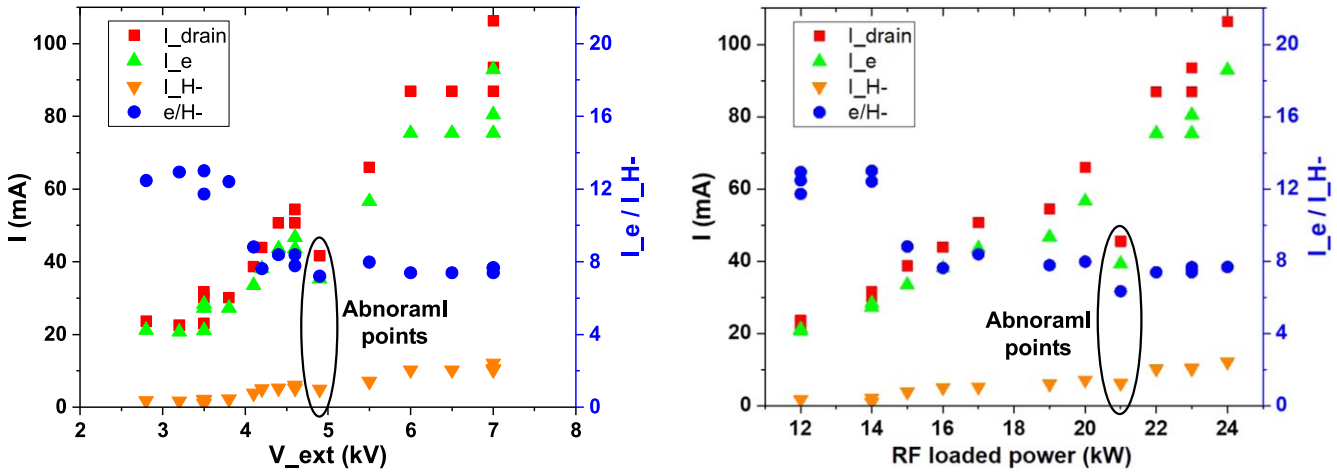

Figure 8. The variation of the drain current (square), the co-extracted electron current (upper triangle), the extracted H− current (lower triangle) and the e/H− ratio (round) were increased with extraction voltage and RF loaded power.

extracted current ratio of electron to ions was decreased with the RF loaded power (from 12 to 7). However, there were some unexpected results that did not accord with such these variation trends. For example, at the RF loaded power was 21 kW, all the extracted currents were unusually low. One of the major reasons was also the unsuitable impendence matching. It induced not only a low coupling power but also a large fluctuation.

4. Discussion and summary

The Hefei utility negative ion test equipment with RF source has been constructed completed and started a commissioning. During the basic RF operation with single driver, a stable plasma discharge has achieved at the required low-pressure and high-power condition. But the loaded power in the long-pulse RF operation was limited because the heat removal of

Faraday shield was insufficient. The self-developed diagnostic systems, OES and CRD, have passed the debugging test and been in-serviced. Combined with other conventional diagnostic systems, they could give the key plasma parameters (e.g. n_e, T_e, n_{H-}) in the source body. The grid conditioning and the double RF drivers operation were carried out at the same time. During the experiment, only the extraction voltage was used and the Cs seeding was not applied. The co-extracted electron current and the extracted H− current were both increased with the RF loaded power and the extraction voltage. But the e/H− ratio had a declining trend from 12 to 7. The highest H-current was above 10 mA. Such an extraction efficiency (i.e. ratio of negative ion current to RF power) without Cs seeding was lower than the other negative ion sources [43].

During the commissioning, the largest problem was the unsuitable impedance matching under the double drivers operation. As mentioned above, it induced an unstable plasma discharge and a series of resulting problems. When searching for the reasons of the unsuitable impedance matching, it was found that the plasma discharge was unbalanced in the two drivers. Hence, there are two major lines in the next experiment campaign of the test equipment. One will pursue a stable low-pressure and high-power plasma discharge with double RF drivers. The other will focus on the characteristics of negative ion extraction with single RF driver.

Acknowledgments

The authors greatly appreciate the discussions with Dr Doo-Hee Chang from KAREI, Daejeon, South Korea. This work was supported by the Key Program of Research and Development of Hefei Science Center, CAS (No. 2016HSC-KPRD002) and National Natural Science Foundation of China (Nos. 11505224, 11505225, 11575240, 11675215, 11675216).

References

[1] Wan Y X *et al* 2017 *Nucl. Fusion* **57** 102009
[2] Wan B N *et al* 2014 *IEEE Trans. Plasma Sci.* **42** 495
[3] Song Y T *et al* 2014 *IEEE Trans. Plasma Sci.* **42** 503
[4] Chan V S *et al* 2015 *Nucl. Fusion* **55** 023017
[5] Berkner K H, Pyle R V and Stearns J W 1975 *Nucl. Fusion* **15** 249
[6] Brown I G 2004 *The Physics and Technology of Ion Sources* 2nd edn (Weinheim: Wiley-VCH Press)
[7] Simonin A *et al* 2016 *New J. Phys.* **18** 125005
[8] McAdams R *et al* 2016 *New J. Phys.* **18** 125013
[9] Heinemann B *et al* 2017 *New J. Phys.* **19** 015001
[10] Hemsworth R S *et al* 2017 *New J. Phys.* **19** 025005
[11] Cartry G *et al* 2017 *New J. Phys.* **19** 025010
[12] Tsumori K and Wada M 2017 *New J. Phys.* **19** 045002
[13] Toigo V *et al* 2017 *Nucl. Fusion* **57** 086027
[14] Wei J L *et al* 2018 *IEEE Trans. Plasma Sci.* **46** 1149
[15] Xie Y H *et al* 2016 *Rev. Sci. Instrum.* **87** 02B302
[16] Xie Y H *et al* 2017 *Fusion Eng. Des.* **114** 72
[17] Jiang C C *et al* 2017 *Fusion Eng. Des.* **117** 100
[18] Speth E *et al* 2006 *Nucl. Fusion* **46** S220
[19] Franzen P *et al* 2007 *Nucl. Fusion* **47** 264
[20] Fantz U *et al* 2009 *Nucl. Fusion* **49** 125007
[21] Kraus W *et al* 2012 *Rev Sci. Instrum.* **83** 02B104
[22] Hu C D *et al* 2015 *Plasma Sci. Technol.* **17** 817
[23] Wei J L *et al* 2016 *Plasma Sci. Technol.* **18** 954
[24] Wei J L *et al* 2016 *Fusion Eng. Des.* **113** 23
[25] Boeuf J P, Fubiani G and Garrigues L 2016 *Plasma Sources Sci. Technol.* **25** 045010
[26] Franzen P *et al* 2011 *Plasma Phys. Control. Fusion* **53** 115006
[27] Wünderlich D *et al* 2016 *Plasma Phys. Control. Fusion* **58** 125005
[28] Bacal M and Wada M 2015 *Appl. Phys. Rev.* **2** 021305
[29] Wimmer C, Schiesko L and Fantz U 2016 *Rev. Sci. Instrum.* **87** 02B310
[30] Yoshida M *et al* 2016 *Rev. Sci. Instrum.* **87** 02B144
[31] Wei J L *et al* 2017 *Fusion Eng. Des.* **117** 93
[32] Gu Y M *et al* 2017 *Fusion Sci. Technol.* **72** 148
[33] Wimmer C, Fantz U and NNBI Team 2016 *J. Appl. Phys.* **120** 073301
[34] Bacal M *et al* 2016 *Rev. Sci. Instrum.* **87** 02B132
[35] Kisaki M *et al* 2014 *Rev. Sci. Instrum.* **85** 02B131
[36] Liang L Z *et al* 2015 *Phys. Scr.* **90** 045603
[37] Fantz U *et al* 2006 *Nucl. Fusion* **46** S297
[38] Kojima A *et al* 2011 *Nucl. Fusion* **51** 083049
[39] Gu Y M *et al* 2018 *Fusion Eng. Des.* **129** 164
[40] Wünderlich D *et al* 2013 *Rev. Sci. Instrum.* **84** 093102
[41] Zhu X M *et al* 2009 *J. Phys. D: Appl. Phys.* **42** 025203
[42] Nakano H *et al* 2016 *J. Instrum.* **11** C03018
[43] Jeong S H *et al* 2016 *Fusion Eng. Des.* **109–111** 186